Neutron-scattering investigations of the Kohn anomaly and of the phase and amplitude charge-density-wave excitations of the blue bronze $K_{0.3}MoO_3$

J. P. Pouget
Laboratoire de Physique des Solides, Bâtiment 510, Université Paris–Sud, 91405 Orsay, CEDEX, France

B. Hennion
Laboratoire Léon Brillouin, CEN Saclay, 91191 Gif-sur-Yvette, CEDEX, France

C. Escribe-Filippini
L.E.P.E.S.—C.N.R.S. Boîte Postale 166 X, 38042 Grenoble, France

M. Sato
Department of Physics, Nagoya University, Chikusa-Ku, Nagoya 464-01, Japan
(Received 6 July 1990)

The quasi-one-dimensional (1D) conductor $K_{0.3}MoO_3$ undergoes a Peierls transition at $T_c = 183$ K. Using cold-neutron scattering, we have succeeded in resolving in frequency and for wave vectors parallel to the chain direction the pretransitional dynamics and the collective excitations of the phase and of the amplitude of the charge-density-wave (CDW) modulation below T_c. The pretransitional dynamics consists of the softening of a Kohn anomaly at the wave vector $2k_F$ together with the critical growth of a central peak in the vicinity of T_c. In addition we observed just above T_c the beginning of a decoupling between the fluctuations of the phase and of the amplitude of the CDW. These features are discussed within the framework of recent model calculations of the dynamics of the Peierls chain. The amplitude mode is clearly observed below T_c with a quasiharmonic frequency ν_A and a damping Υ_A, which perfectly agree with that found in a previous Raman scattering investigation of blue bronze. By continuity with the behavior of the pretransitional fluctuations, ν_A does not soften at T_c. The dispersion of the phase mode has also been measured in the chain direction near T_c. In this temperature range the phason velocity is quite high (about one-tenth of the Fermi velocity), giving a CDW mass enhancement of ~ 100. High-resolution measurements show that the phason response is overdamped at $2k_F$ with a small gap whose estimated value corroborates that recently found for the high-frequency pinning mode of the blue bronze by millimeter-wavelength-range conductivity measurements.

I. INTRODUCTION

Since the discovery more than 15 years ago of the Peierls transition[1] and of the formation of a giant Kohn anomaly[2] in the acoustic-phonon spectrum of the one-dimensional (1D) conductor $K_2Pt(CN)_4Br_{0.3}\cdot xH_2O$ (KCP), a considerable number of studies have been devoted to the physics of the charge-density waves (CDW's) stabilized by the Peierls transition and to the manifestation of their collective behavior.[3]

In the classical limit Peierls instability arises from first-order coupling between the 1D electron gas, whose electron-hole polarizability diverges for the $2k_F$ wave vector, and the phonon field. Through the excitation of real electron-hole pairs, a Kohn anomaly is formed in a given phonon branch whose softening drives the CDW instability. In the presence of 1D instability, the interchain coupling between CDW's leads to a structural transition at a finite temperature T_c in real systems. Below T_c the structural distortion consists in a modulation wave of the high-temperature lattice positions:

$$u(\mathbf{r}) = A\cos(\mathbf{q}_c\mathbf{r}+\varphi)\ , \tag{1}$$

where the in-chain component of the wave vector of the modulation $\mathbf{q}_c$ is $2k_F$. This component, related through the Fermi wave vector k_F to the 1D band filling, is generally in incommensurate relation with the in-chain reciprocal wave vectors of the high-temperature lattice. The low-energy excitations of the incommensurate modulation, or that of the CDW ground state, are those of the amplitude A and phase φ in (1). They give rise to two branches called, respectively, amplitudon and phason in the phonon spectrum below T_c. Such branches have been measured by inelastic neutron scattering in incommensurate insulators like the biphenyl[4] and $ThBr_4$,[5] but could not be unambiguously found by these techniques in low-dimensional conductors, although Raman[6,7] and infrared[8–10] measurements suggest the presence of such excitations. The presence of a phase degree of freedom below T_c is a key feature governing the physical properties associated with the CDW sliding.[3] Another important question concerns the way by which the phase and

amplitude excitation branches emerge from the Kohn anomaly. Is the mean-field-like scenario, observed in incommensurate insulators[11] and shown in Fig. 1(a), still valid or does the decoupling between the phase and amplitude degrees of freedom already occur during the pretransitional fluctuations, as schematically illustrated by Fig. 1(b), which summarizes recent numerical calculations of the dynamics of the Peierls chain?[12] Although earlier neutron investigations of KCP (Refs. 13 and 14) suggest the latter scenario, its basic features could not be studied in detail because of the frozen dynamics probably due to the intrinsic disorder present in this class of materials. Crystals of other 1D conductors like tetrathiafulvalene-tetracyanoquinodimethane were too small to allow a detailed investigation of the dynamics of Peierls transition.[13,15] In contrast, blue bronze, which forms well-ordered single crystals of sizable volume and which exhibits a well-defined Peierls transition, offers the opportunity of a complete study of the dynamics of the pretransitional fluctuations and the collective excitations of the CDW ground state.

The molybdenum blue bronzes $A_{0.3}MoO_3$, where A is a monovalent metal like K, Rb, or Tl are quasi-one-dimensional conductors.[16] They undergo at $T_c = 183$ K a second-order Peierls metal-semiconductor phase transition toward a CDW-modulated structure characterized by the wave vector $\mathbf{q}_c = (1, 2k_F, 0.5)$,[17] where the in-chain component $2k_F$, close to $\frac{3}{4}$, decreases slightly for increasing temperatures.[18–23] In its semiconducting phase blue bronze shows interesting transport properties associated with the sliding of the incommensurate CDW modulation above a sharp threshold field.[24] Such a CDW sliding has been directly observed by ^{87}Rb NMR in $Rb_{0.3}MoO_3$.[25]

The spatial aspects of the pretransitional fluctuations of the Peierls transition of $K_{0.3}MoO_3$ have been measured by x-ray diffuse scattering.[20] In particular, it has been shown that because of a sizable coupling along $\mathbf{a}+2\mathbf{c}$ (in the layers of MoO_6 octahedra), the CDW fluctuations are basically 2D from room temperature to about 200 K, the temperature below which 3D critical fluctuations develop.[20,26] These x-ray diffuse scattering data have been again analyzed in the classical limit and in the random-phase approximation of the lattice fluctuations.[27] From the behavior of the $2k_F$ CDW response function and the in-chain CDW correlation length, the temperature dependence of the susceptibility associated with the critical distortion u and electron-hole polarizability have been deduced. These findings will be considered later in the discussion of our neutron results.

Earlier neutron investigations of $K_{0.3}MoO_3$ and $Rb_{0.3}MoO_3$ above T_c provide evidence of a Kohn anomaly in a low-lying phonon branch.[18,21,22] But the presence of several phonon branches of low frequency makes its assignment to a peculiar phonon mode particularly difficult. It is not clear if the Kohn anomaly belongs to an acousticlike or opticlike phonon branch. According to the structural determination of the main directions of displacement of the Mo(2) and Mo(3) atoms below T_c,[23,28,29] it is probably polarized in the layers of MoO_6 octahedra. Figure 2 shows some low-lying phonon branches of $K_{0.3}MoO_3$ with, in one of them, the critical Kohn anomaly quite well developed at 230 K. A more complete investigation of the dispersion of the low-lying phonon branches of blue bronze will be the object of a further publication. Earlier neutron studies[18,22,23] have provided clear evidence of the softening of the Kohn anomaly and the critical growth of a central peak in frequency when the Peierls critical temperature T_c is ap-

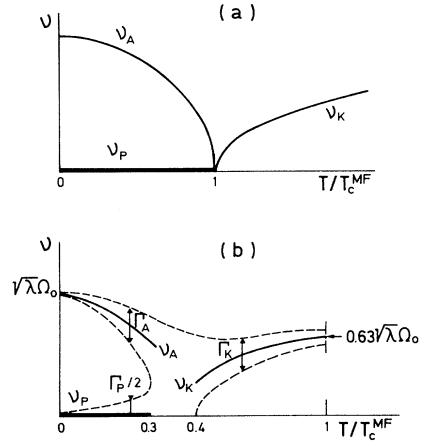

FIG. 1. (a) Mean-field behavior of the frequency of the Kohn anomaly (ν_K), the amplitude node (ν_A), and the phase mode (ν_P) for the critical $2k_F$ wave vector, as a function of the temperature. (b) Schematic representation of the temperature dependence of the maxima in frequency (ν_i), full width at half maximum (Υ_i) of the response function $S(2k_F, \nu)$ of the Peierls chain (adapted from the numerical simulations of Ref. 12).

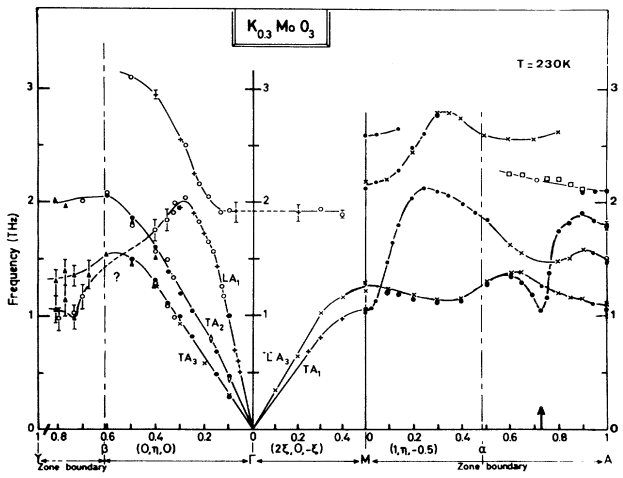

FIG. 2. Dispersion of some low-lying phonon branches of $K_{0.3}MoO_3$. The location of the Kohn anomaly at 230 K is shown by an arrow.

proached from above. Here we present a detailed study of this softening using cold-neutron scattering, which enable us for the first time to resolve the Kohn anomaly in frequency (ν) and for wave vectors parallel to the chain direction (q_b).

A second goal of this paper is to provide a quantitative study of the low-frequency structural excitations of the incommensurate modulation of $K_{0.3}MoO_3$ below T_c. As the CDW arises from a single **q** modulation of the atomic positions, these excitations consist of a single-phase mode and a single-amplitude mode.[11] Evidence for amplitude-mode excitations were provided by Raman scattering.[17] This mode was also briefly mentioned in earlier studies,[23,30] but its detailed ν-versus-q_b study has not been performed. We have also briefly mentioned in earlier reports[30,31] the observation, by means of neutron scattering, of the phase mode in blue bronze. Full details of its investigations will be given here. In the presence of pinning, the transverse-phase excitations can be generally observed by far-infrared reflectivity measurements. Evidence for such infrared excitations were claimed by several groups,[9,10] with, however, discrepancies in the true value of the pinning frequency. Recent studies show, in fact, that the dynamics of the pinned CDW of blue bronze is quite complex with a well-defined high-frequency pinning mode around 0.1 THz and a distribution of low-frequency pinning modes.[32] This question will be also considered here from high-resolution cold-neutron measurements.

II. EXPERIMENTAL

The neutron measurements were carried out on the three-axis spectrometers $4F_1$ and $4F_2$ installed on a cold-neutron source at the Orphee reaction of the Laboratoire Léon Brillouin at CEN Saclay. A frequency range up to 2.3 THz has been investigated around the $(5,2k_F,2.5)$ and $(1,4-2k_F,\overline{0.5})$ positions in the reciprocal space. A short report of the results obtained around $(5,2k_F,2.5)$ has been given in Ref. 31. But in that zone two more phonon branches near 1.3 and 1.5 THz were visible and their presence seriously hampered the data analysis above 1 THz. These two branches are not observed around $(1,4-2k_F,\overline{0.5})$, and we succeeded in obtaining data allowing accurate quantitative analysis.

The $K_{0.3}MoO_3$ material used in this study was grown at the Institute for Molecular Science (Okazaki, Japan). It consists of a single crystal of about 5 cm^3 accompanied by a few small crystallites. These crystallites give rise to parasitic contributions, which appeared as low-intensity anomalies, but their low intensities allowed to incorporate them in a mere enhancement of the background. The Peierls critical temperature of the sample has been determined to be $T_c=183$ K, the temperature at which the satellite intensity vanishes. The incommensurate component of the modulation wave vector $2k_F$ is temperatue dependent and was found to vary between $(0.748\pm0.001)b^*$ at 100 K and $(0.736\pm0.001)b^*$ at 175 K, in agreement with earlier reports.

III. RESULTS AND ANALYSIS

A set of measurements have been carried out in the scattering plane $(b^*,2a^*\text{-}c^*)$ in a frequency range from -0.2 to -2.3 THz by steps of -0.1 THz from $\mathbf{q}=(1,3.15,\overline{0.5})$ to $(1,3.40,\overline{0.5})$. Data were collected at 230, 210, and 190 K above T_c, and 175, 160, and 130 K below T_c. Constant incoming wave vectors $k_I=1.8$ and 2 $Å^{-1}$ have been used. Horizontal collimation $-/-/60'/40'/40'$ provided a frequency resolution varying between 0.07 and 0.15 THz full width at half maximum (FWHM). The frequency range from -0.2 to -1.6 THz was investigated with $k_I=1.8$ $Å^{-1}$ and from -1 to -2.3 THz with $k_I=2.0$ $Å^{-1}$. This allowed a cross-check of the results to prevent them from artifacts related to higher-order contamination, even though the use of a cold source and a double monochrometer strongly decreases that risk. On the other hand, this also allowed a check of the stability of the solutions given by the fitting procedure in the data analysis.

To present the results in their qualitative as well as quantitative aspects, a three-dimensional display of the results is done in Fig. 3. In order to get a readable presentation, raw data have been smoothed along both the ν and q_b axes, each point being weighted by its immediate neighbors.

The main features of the thermal evolution can thus be pointed out. Above T_c the Kohn anomaly is clearly seen as a dip in a phonon branch, whose frequency decreases with the temperature [Figs. 3(a) and 3(b)]. Below T_c two excitations may be distinguished, a high-frequency one, looking like an optical mode, and a steep acoustic-like one, mainly seen as a ridge at the q position of the satellite [Fig. 3(c)].

In order to get quantitative information from these data we analyze them as follows.

A. $T>T_c$

In the absence of a specific analytical formula for the neutron-scattering cross section, taking properly into account the fluctuations of the Peierls chain, especially in the vicinity of T_c (see Sec. IV); we have used the response function of a damped harmonic oscillator:

$$S(q,\nu)=|F_q|^2\frac{\nu}{1-\exp(-h\nu/k_BT)}\frac{\Upsilon_q}{(\nu^2-\nu_q^2)^2+\nu^2\Upsilon_q^2}\ . \tag{2}$$

For each q value the data have been fitted to a calculated intensity resulting from the convolution of $S(q,\nu)$ with the resolution function of the spectrometer, with ν_q, Υ_q, and $|F_q|^2$ as adjustable parameters.

Because of the focusing effect, the slope $\delta\nu_q/\delta q$ of the dispersion relation plays an important role in the determination of Υ_q. To account for that, the fitting procedure for the whole set of q values has been repeated recursively to get a consistent set of ν_q and $\delta\nu_q/\delta q$ values. By this way we got the q dependence of ν_q, Υ_q, and $|F_q|^2$ at a given temperature. We found that, within the error bars, $|F_q|^2$ was slowly and continuously varying in the q

range of observation and was temperature independent, which is quite normal behavior. The fitting was then repeated with fixed $|F_q|^2$ for q values where the damping of the mode yielded strong correlations between adjustable parameters. With this reasonable assumption we got more precise values for ν_q and Υ_q. The results are reported at 230 K in Fig. 4(a) and at 190 K in Fig. 4(b), where fixed $|F_q|^2$ values are indicated by crosses instead of open circles.

Figures 3(a), 3(b), and 4 show that we have been able to resolve in frequency and for the reciprocal wave vector q_b the Kohn anomaly of blue bronze. The Kohn anomaly shows a minimum frequency (ν_K) and a maximum damping (Υ_K) for $q_0 = 2k_F$. When T decreases toward T_c, ν_K decreases and Υ_K increases. The temperature dependence of ν_K^2 and Υ_K are reported in Fig. 5 together with earlier results obtained on a different crystal (data from fig. 3 in Ref. 22 and obtained on the three-axis spectrome-

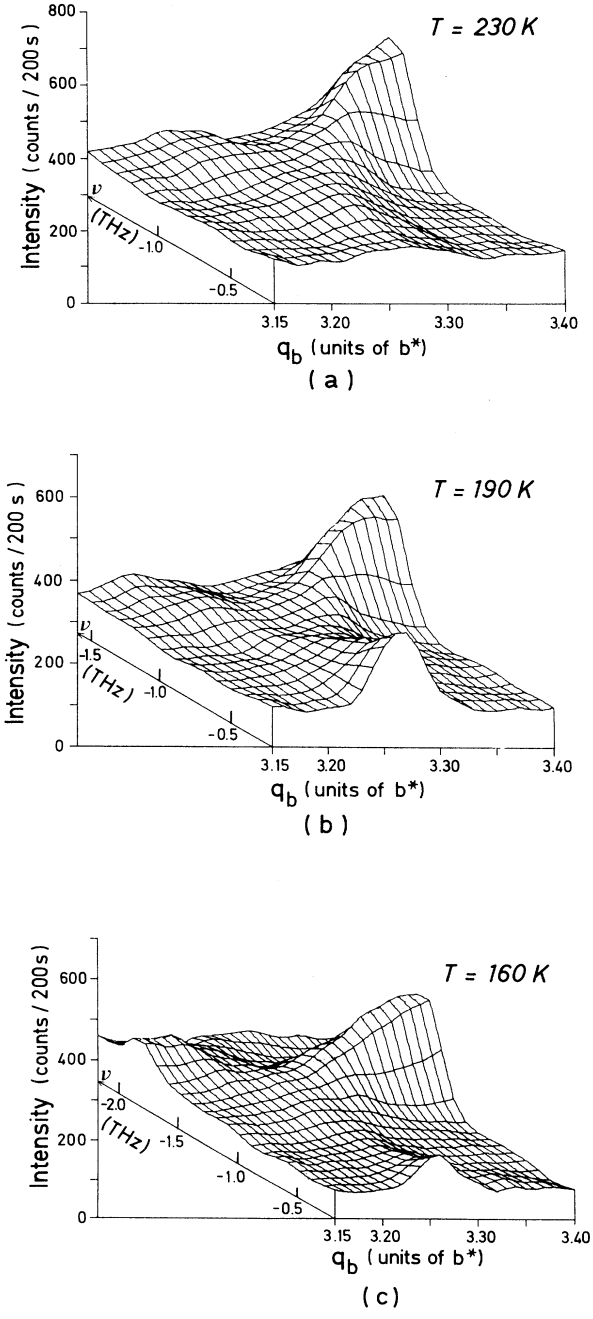

FIG. 3. Neutron-scattered intensity in function of the in-chain wave-vector component q_b and of the frequency ν for the reciprocal positions $(1, q_b, \overline{0.5})$ at (a) 230 K, (b) 190 K, and (c) 160 K. These three-dimensional displays are raw data smoothed along ν and q_b as described in the text.

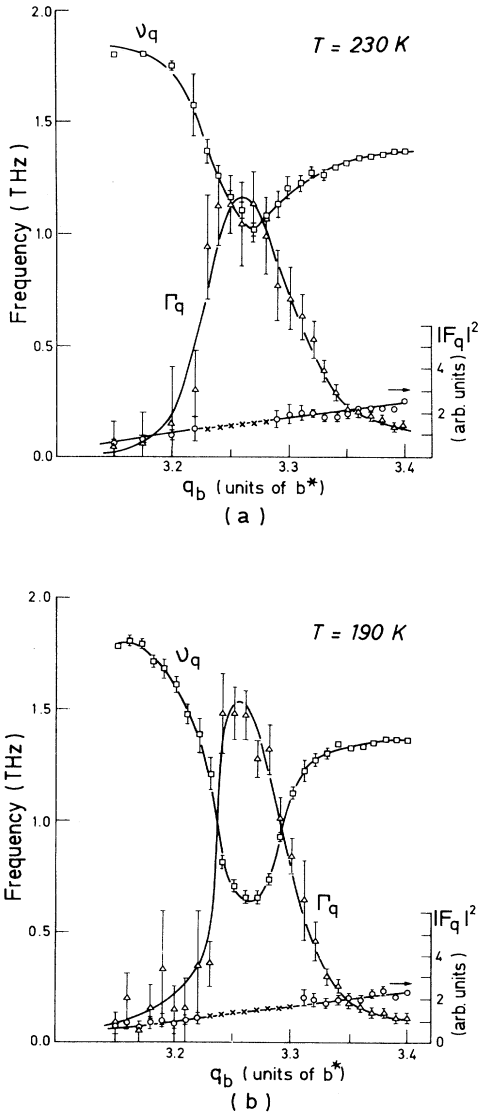

FIG. 4. Quasiharmonic frequency (ν_q), damping (Υ_q), and square of the structure factor ($|F_q|^2$) deduced from the damped harmonic-oscillator fit of the Kohn anomaly measured at (a) 230 K and (b) 190 K in $(1, q_b, \overline{0.5})$.

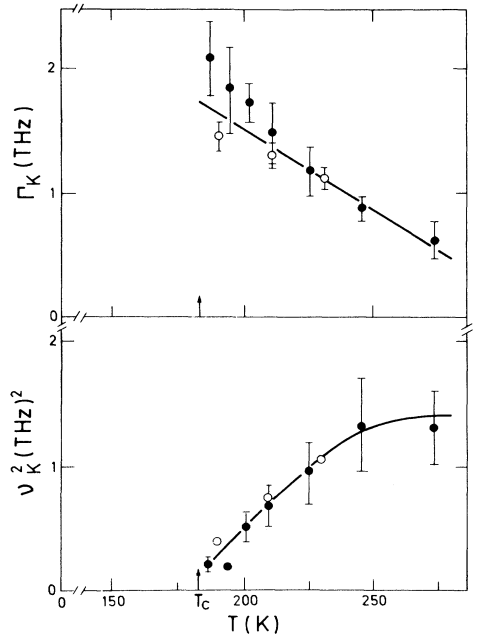

FIG. 5. Temperature dependence of the square of the quasiharmonic frequency (ν_K^2) and of the damping (Υ_K) of the Kohn damping. The open symbols are from the present cold-neutron study and the solid symbols are from the thermal neutron study of Ref. 22 (a shift of temperature of 4.5 K has been applied to the three low-temperature points of this last study in order to have a common T_c for the two sets of data).

ter $2T$ installed on a thermal neutron source). These earlier results had been obtained through another data analysis, because at that time we had not resolved the q dependence of the Kohn anomaly and assumptions were needed concerning the q dependence of the mode in the vicinity of ν_K as well as the temperature independence of $|F_q|^2$. These assumptions have now been proven by the present measurements, and both determinations agree quite well, as shown by Fig. 5.

Υ_K increases by a factor 3 between room temperature and T_c. ν_K^2 decreases almost linearly with temperature but does not seem to tend toward zero at T_c. Besides that, the observation of the critical growth of a central peak near T_c shows that the pretransitional dynamics of $K_{0.3}MoO_3$ is more complex than a mere mode softening. The validity of a damped harmonic oscillator to describe $S(q,\nu)$ in quasi-1D systems may be questioned, especially in the vicinity of T_c when the fluctuations are quite strong and when decoupling between the fluctuations of the phase and amplitude of the order parameter are expected to occur. These questions will be considered in Sec. IV.

B. $T < T_c$

Two excitations are now seen, one acousticlike starting from the incommensurate satellite position (the phason) and one optical-like (the amplitudon). As seen in Fig. 3(c); the phase mode is not very intense around the $(1,4-2k_F,\overline{0.5})$ reciprocal position and the scattering is centered on the satellite position. So in order to decrease the number of adjustable parameters we have only fitted the amplitudon mode, the phason signal being treated as a slight enhancement of the background in the vicinity of the satellite position. Another set of measurements have been carried out in order to get more specific information on the phase mode, especially around the $(5,2k_F,2.5)$ reciprocal position.

1. *Amplitude mode*

The same analysis as in Sec. III A has been performed. We found the same behavior for $|F_q|^2$ so that the same constraint could be applied. The results for ν_q, Υ_q, and $|F_q|^2$ as a function of q_b are reported at 160 K in Fig. 6(a) and at 130 K in Fig. 6(b). ν_q shows only a slight anomaly with a corresponding maximum of Υ_q at $2k_F$ (ν_A and Υ_A respectively). The values of $|F_q|^2$ are quite similar to those found above T_c.

Figure 7 shows the temperature dependence of ν_A and Υ_A together with values taken from the Raman data of Ref. 7. In the temperature range where the data overlap, there is very good agreement between the neutron- and Raman-scattering determinations. This agreement, as well as the continuity of $|F_q|^2$ through the Peierls transition, prove that we have really observed the amplitude mode by neutron scattering. However, it is interesting to remark that, at T_c, ν_A does not soften to zero, and that Υ_A shows a stronger temperature dependence than ν_A near T_c. These aspects, unexpected for a classical second-order phase transition [see Fig. 1(a)], will be discussed in Sec. IV.

2. *Phase mode*

Two steep acousticlike phonon branches which seem to start from the satellite reflection have been detected in the vicinity of $(1,4-2k_F,\overline{0.5})$ and $(5,2k_F,2.5)$ reciprocal positions. Evidence for such excitations in the first zone are shown in Fig. 3(c). However, because of their strongest intensity, a better characterization has been done in the second zone. Figure 8 shows, in this zone, constant frequency scans along q_b from $\nu=-0.4$ to -1 THz at 175 K. When $|\nu|$ is increased one observes a continuous broadening of the neutron response and its splitting into two components above -0.8 THz. For low frequencies $+q_P$ and $-q_P$ peaks are not resolved and we only observe a scattering with a maximum at the satellite position q_s. When the frequency is increased, this peak broadens and is nearly resolved into two components at -1 THz. As already explained, measurements at higher frequencies are unreliable because of the presence of other phonon branches and the proximity of the damped amplitudon.

The analysis of these data with two harmonic oscillators centered at $\pm q_P$, yields the linear dispersion reported on the right side of Fig. 8. Peak positions are deduced from the calculated profile, which is given by the continuous line on the left side. The dispersion corresponds to

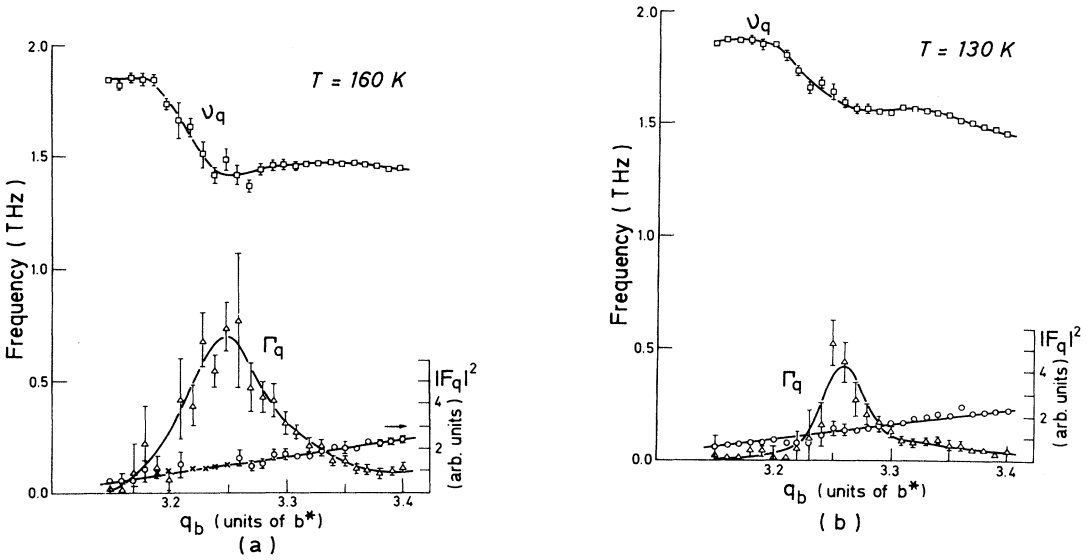

FIG. 6. Quasiharmonic frequency (ν_q), damping (Υ_q), and square of the structure factor ($|F_q|^2$) deduced from the damped harmonic-oscillator fit of the amplitude mode measured at (a) 160 K and (b) 130 K in $(1,q_b,\overline{0.5})$.

$$\nu = v_\varphi \eta \ . \tag{3}$$

with $\eta = |q_b - 2k_F|$ and $v_\varphi = 21 \pm 3 \times 10^3$ m/s.[33] The velocity v_φ is very high: 2 times larger than that of the steepest acoustic mode (longitudinal-acoustic mode propagating along b^*; LA_1 in Fig. 2). Because of the high value of the slope, effects due to the damping of the phonon do not change drastically the estimate of the slope given above.

It is also interesting to remark that v_φ amounts to the square root of the curvature of the Kohn anomaly $\sqrt{\Lambda_\parallel}$ deduced from the results of Fig. 4(b) of Sec. III A, when the q_b dependence of the Kohn anomaly in the vicinity of its minimum is expressed as

$$\nu(q)^2 = \nu_K^2 + \Lambda_\parallel \eta^2 \ . \tag{4}$$

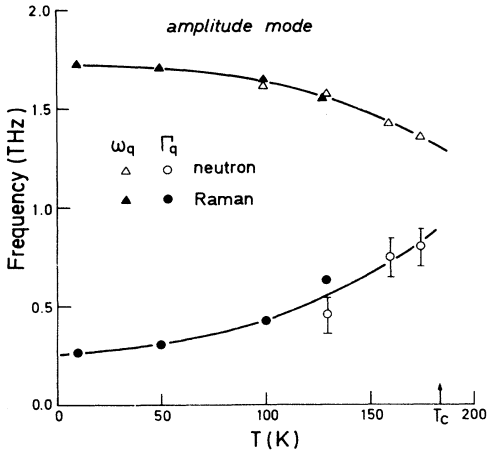

FIG. 7. Temperature dependence of the quasiharmonic frequency (ν_A) and damping (Υ_A) of the amplitude mode. The open symbols correspond to the present neutron study, and the solid symbols correspond to the Raman study of Ref. 7.

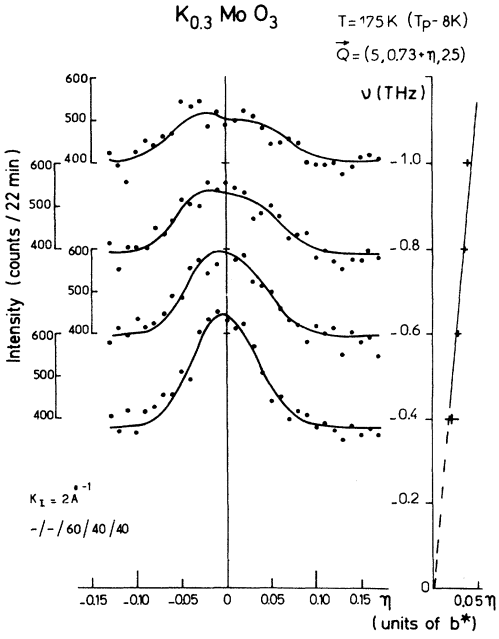

FIG. 8. Neutron scans at constant frequency from $\nu = -0.4$ to -1 THz around $\mathbf{Q} = [5, 0.73+\eta, 2.5]$ at 175 K. The solid line is the result of the convolution by the experimental resolution of two harmonic oscillators centered at $\pm q_P$. q_P deduced from such a fit is indicated by a cross on the right side of the figure for each value of ν scanned.

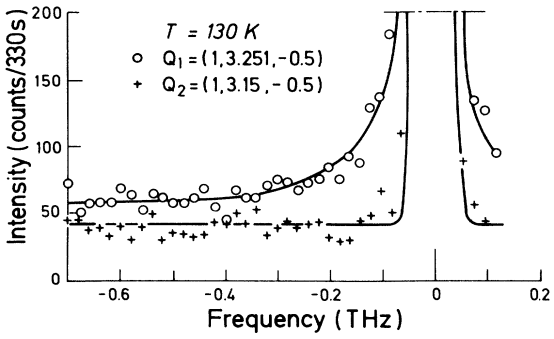

FIG. 9. Frequency scans at 130 K at the position of the satellite reflection, $\mathbf{Q}_1=(1,3.251,\overline{0.5})$, and slightly off this position, $\mathbf{Q}_2(1,3.15,\overline{0.5})$, showing, by difference, the net increase of scattering cross section corresponding to the phason branch. The solid line gives the fit of the $\mathbf{Q}_1$ data by a damped harmonic oscillator with $\nu_P=0.2$ THz and $\Upsilon_P=0.8$ THz.

At 190 K one gets, from Fig. 4(b), $\sqrt{\Lambda_\parallel}\cong 19.5\times 10^3$ m/s.[33] The correspondence between v_φ and $\sqrt{\Lambda_\parallel}$ is expected from the phenomenological theory of the phason[11] and by the continuity of $S(q,\nu)$ for a second-order incommensurate transition. However, for temperatures lower than 175 K, a stiffening of v_φ will certainly occur because of the reduction of the screening effects of the Coulomb forces involved in the longitudinal deformations of the phase of the CDW. Such screening effects due to normal carriers excited through the Peierls gap, decrease with the decreasing number of such carriers at low temperature.[34] Experiments to determine the temperature dependence of v_φ are underway.

If Fig. 8 provides evidence for phase excitations of the incommensurate modulation of $K_{0.3}MoO_3$ for $\nu\geq 0.4$ THz, it is not demonstrated that the dispersion (3) holds for small values of ν. For the purpose of detecting the presence of an eventual phason gap at $\eta=0$ and to study the damping of the phason mode, we have performed between 130 and 175 K high-resolution scans at $\mathbf{Q}_1=(1,3.251,\overline{0.5})$ from 0.04 to 0.7 THz with $k_I=1.55$ Å^{-1} (beryllium filter) and horizontal collimations $-/-/60'/40'/40'$ achieving a frequency resolution of 0.035 THz (FWHM). In order to separate the contribution of the phason branch from the background and the contamination due to the proximity of the satellite reflection, we have performed the same scan at a slightly different wave vector $\mathbf{Q}_2=(1,3.15,\overline{0.5})$. Figure 9 shows two such scans at 130 K. There is a net increase of scattering for the scan performed at $\eta=0$. A similar increase of intensity was previously reported between ν scans performed for $\mathbf{Q}_1=(5,0.74,2.5)$ and $\mathbf{Q}_2=(5,0.79,2.5)$ in Ref. 31 (the shoulder found at about 0.5 THz in this work disappears for scans performed with better statistics).

The data of Fig. 9 do not give evidence for such a gap. Nevertheless, the data have been tentatively analyzed with the assumption of a damped frequency gap and a linear dispersion with the slope previously estimated. The least-squares fit gives, at $2k_F$, an overdamped phason with a damping of $\Upsilon_P=0.8\pm 0.2$ THz and a frequency gap of $\nu_P=0.2\pm 0.1$ THz. These values do not vary within experimental errors between 130 and 175 K. The damping constant Υ_P agrees with that previously obtained for the amplitude mode in the same temperature range (see Fig. 7). The quasi-harmonic-gap frequency ν_P, sizably smaller than Υ_P, is quite inaccurate. However, it is interesting to remark that our value of ν_P is close to that of the high-frequency pinning mode ~ 0.1 THz obtained from millimeter-wavelength-range conductivity measurements.[32,35] Our $2k_F$ overdamped phason mode has also parameters close to that ($\nu_P\sim 0.1$ THz, $\Upsilon_P\sim 0.5$ THz) of the far-infrared response reported in Ref. 10.

IV. DISCUSSION

By cold-neutron scattering we have succeeded in resolving in frequency and for in-chain wave vectors the pretransitional dynamics and CDW collective excitations of a quasi-1D conductor undergoing a Peierls transition. In particular, it has been clearly observed (see, in particular, the close correspondence between v_φ and $\sqrt{\Lambda_\parallel}$ on each side of T_c) that the softening of the Kohn anomaly leads to the formation of the phase mode. Such behavior is expected for a displacive phase transition, in particular, in the case of mean-field theory.[11] Figure 1(a) gives schematically, for such a model, the temperature dependence at $2k_F$ of ν_K, ν_A, and ν_P (in this figure the additional effect of pinning of the phase-mode frequency have been neglected; thus $\nu_p=0$). Mean-field theory predicts, in particular, that the amplitude mode also softens at the critical temperature.[36] Such behavior is not corroborated by our data (Fig. 7). If one assumes a mean-field-like temperature dependence for the quasiharmonic frequency of the amplitude mode under the form

$$\nu_A^2\sim(T-T_1)\ , \tag{5}$$

one would expect, from the data of Fig. 7, its vanishing at about $T_1\sim 320$ K.[30] This temperature is about 2 times larger than the Peierls critical transition temperature T_c. However, it is interesting to remark that T_1 is not too far from the mean-field Peierls temperature of the blue bronze $T_c^{\rm MF}$) that can be deduced from the BCS relationship $\Delta_0=1.78k_BT_c^{\rm MF}$ knowing the half Peierls gap at 0 K [$\Delta_0\sim 50$ meV (Ref. 37) to 75 meV (Ref. 16)]. This seems to indicate that when the phase and amplitude excitations of the CDW are well decoupled, as is the case below T_c, the amplitude excitations are controlled by the mean-field behavior of the distorted Peierls chain. The delicate point concerns the description of the merging of the phase and amplitude excitation branches above T_c.

In agreement with the second-order nature of the Peierls transition of blue bronze, the raw data (Fig. 3) show that $S(q,\nu)$ behaves continuously at T_c. This means that the amplitude mode does not appear abruptly at T_c at a finite frequency of about 1.3 THz. More likely, the branch of amplitude excitation must emerge continuously from the Kohn anomaly above T_c.

In order to describe more precisely the thermal evolu-

tion of $S(q,\nu)$ through the Peierls transition, we have reported in Fig. 10 for $q=2k_F$ the behavior of the quasiharmonic frequency ν_i and of the frequencies $\nu_i+\Upsilon_i/2$ for the Kohn anomaly ($i=K$, data of Fig. 5), the amplitude mode ($i=A$ data of Fig. 7), and the phase mode ($i=P$); in the case of an underdamped harmonic oscillator $\nu_i\pm\Upsilon_i/2$ is the frequency of the half-intensity. This figure shows by continuity that the amplitude mode seems to emerge from the Kohn anomaly on its high-frequency flank around 230 K. This finding, previously noted in Ref. 30, is now corroborated by measurements performed just above T_c. In particular, Fig. 3(b), obtained at 190 K (T_c+7 K), shows above the dip of the Kohn anomaly a branch of weak intensity at a frequency of about 1.3 THz, which corresponds to that at which amplitude excitations are observed just below T_c. We have tried to fit these data by two damped harmonic oscillators: a low-frequency one, corresponding to the bottom of the Kohn anomaly, and a high-frequency one, corresponding to the remaining trace of the amplitude mode above T_c. However, because of the weak intensity of this last mode, we have not succeeded in obtaining a reasonable convergence of the oscillator parameters. Although in the vicinity of T_C the raw data shows that $S(q,\nu)$ is peaked at two frequencies, the strongest intensity of the low-frequency response, in the $(1,4-2k_F,\overline{0.5})$ reciprocal position, justifies the analysis of the softening of the Kohn anomaly performed in Sec. III A.

Recently, the response function $S(q,\nu)$ of the Peierls chain has been obtained by numerical simulation.[12] The main results of such a calculation are schematically illustrated by Fig. 1(b). It gives the temperature behavior of

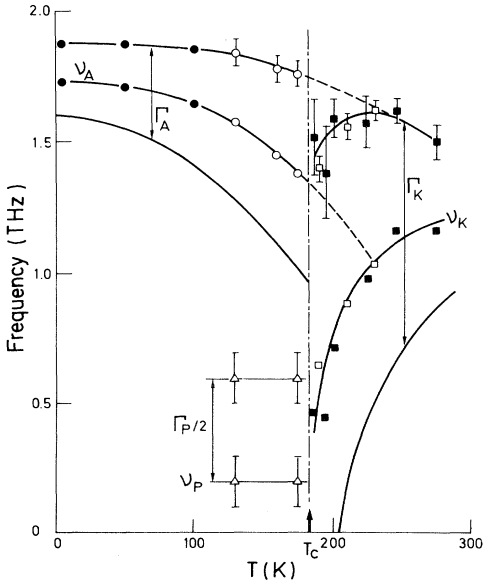

FIG. 10. Temperature dependence of the quasiharmonic frequency ν_i and the frequencies $\nu_i\pm\Upsilon_i/2$ for the Kohn anomaly ($i=K$), amplitude mode ($i=A$), and phase mode ($i=P$) of blue bronze at $2k_F$, using the damped harmonic-oscillators parameters obtained in our analysis of the neutron data and those of Ref. 7 for ν_A and Υ_A below 100 K.

the maxima of $S(2k_F,\nu)$ and, in the spirit of Fig. 10, of the FWHM of the corresponding peak width. At $T_c^{\rm MF}$, in the quartic regime of fluctuations, a numerical solution is known.[38] When the temperature decreases, the softening of the quasiharmonic frequency (ν_K) of the Kohn anomaly and the increase of its damping (Υ_K) due to anharmonicity leads to an overdamped response near $0.4T_c^{\rm MF}$. At about $0.3T_c^{\rm MF}$ the mode of the fluctuation of the amplitude begins to emerge at a finite frequency (ν_A) from the overdamped response and becomes more separated from the phase mode as the temperature decreases. The separation is caused both by the increase of the quasiharmonic frequency ν_A and by the decrease of the damping Υ_A and Υ_P of the two degrees of freedom, when the temperature decreases below 0.3 $T_c^{\rm MF}$ (in the classical limit Υ_A and Υ_P decrease linearly with T). At $T=0$ K the frequency of the amplitude mode is given by mean-field theory.[39] In real systems this 1D behavior is perturbated by the 3D coupling. In the case of weak interchain interactions, the 3D coupling leads to a true Peierls transition at about $T_c^{\rm MF}/3$, with nearly no change in the dynamics. A stronger 3D coupling diminishes the amplitude fluctuations, i.e., increases their characteristic frequency, which leads to a better decoupling between the fluctuations of the phase and amplitude of the CDW. In that case the 1D description remains qualitatively valid, but the characteristic temperatures are higher than those of the pure 1D description. This last situation is probably encountered in blue bronze because the temperature of decoupling between the phase and amplitude excitations $\sim 0.5T_c^{\rm MF}$ (i.e., between 190 and 230 K; see Fig. 10) is slightly higher than that of the isolated Peierls chain $\sim 0.3T_c^{\rm MF}$ [Fig. 1(b)]. Correlation length measurements show that the interchain coupling is especially important in the layer of MoO_6 octahedra, but remains weak along $2a^*$-c^* between two successive layers.[20,26,30,40]

Within the present accuracy of our analysis, summarized by Fig. 10, the decoupling temperature below which the amplitude mode begins to emerge from the Kohn anomaly corresponds to the temperature (~ 220 K) at which pretransitional resistive fluctuations are observed on the electrical conductivity[41] and where the digging of the pseudogap begins to affect seriously the divergence of the electron-hole polarizability.[27] It is also close to the temperature (~ 200 K) at which the crossover to the regime of 3D critical fluctuations is observed by x-ray diffuse scattering[20,26] and by T_1 NMR relaxation.[42]

In the quartic regime of the fluctuations, at $T_c^{\rm MF}$, it has been shown[38] that the frequency of the minimum of the Kohn anomaly, $\nu_K^{\rm MF}$, is related to that of the amplitude mode frequency at zero temperature ν_A^0 through the relationship

$$\nu_K^{\rm MF}=0.63\nu_A^0 \ . \tag{6}$$

With $\nu_A^0=1.73$ THz (Ref. 16) (see also Fig. 7), expression (6) gives $\nu_K^{\rm MF}=1.09$ THz. This frequency is in good agreement with that measured at room temperature, close to $T_c^{\rm MF}$: $\nu_K=1.16\pm 0.14$ THz (see Fig. 5).

Together with phonon softening the damping increases (Fig. 5). The maximum of damping occurs for the wave

vector at which the quasiharmonic frequency shows a minimum, i.e., the bottom of the Kohn anomaly (Fig. 4). The damping is due to anharmonicity. In the numerical simulation it comes from the quartic term of the Lagrangian.[12] In the quartic regime of fluctuation at T_c^{MF}, it is surprisingly found[38] that the $2k_F$ critical phonon remains well defined in frequency with a full width of about $\frac{1}{5}$ its frequency. This gives for blue bronze a full width of about 0.23 THz. This value agrees roughly (i.e., within a factor 2) with the damping estimated from the extrapolation at T_c^{MF} of the temperature dependence of Υ_K. Our determination of Υ_K^{MF} is, however, quite inaccurate because there are large uncertainties on the experimental values of Υ_K (Fig. 5) and on the exact value of T_c^{MF}.

The increase of damping Υ_K with the decrease of the quasiharmonic frequency ν_K leads to an overdamped Kohn anomaly at low temperature. Such a situation is observed between about 210 K in blue bronze (Fig. 10) (between $(0.3-0.4)T_c^{MF}$ in the numerical simulation [Fig. 1(b)] (Ref. 12)). The upper temperature coincides roughly with that at which the amplitude mode begins to be distinguished in the pretransitional fluctuations. Below 210 K the overdamped behavior of the Kohn anomaly in blue bronze recalls that observed in KCP over the whole temperature range of measurements.[13,14] Because of its enhanced overdamped behavior, the Kohn anomaly could not be studied quantitatively in KCP.

Above T_c the square of Kohn anomaly frequency, ν_K^2, decreases almost linearly in temperature. However, our analysis of the data shows that the frequency does not soften completely at T_c. The linear extrapolation of the data of Fig. 5 gives, at T_c, $\nu_K \sim 0.5-0.3$ THz. Such a value corresponds roughly to the frequency of the gap of the phase mode ($\nu_p = 0.2 \pm 0.1$ THz) previously estimated below T_c. X-ray diffuse scattering measurements of the inverse susceptibility associated with the order parameter shows a temperature dependence analogous to that of ν_K^2,[27] except in the near vicinity of T_c where a divergence characterized by the critical exponent γ ($n=2$, $d=3$) is measured.[26] In the pretransitional dynamics this behavior is brought on by the critical divergence of a quasielastic central peak. Such a central peak is observed on our data and by earlier neutron investigations.[18,22] This elastic response in frequency can be detected for temperatures as high as 225 K. This additional response is not shown by the simulations of the fluctuations of the Peierls chain in the underdamped regime of the Kohn anomaly.[12] $2k_F$ static Friedel oscillations induced by defects or impurities[43] contribute certainly to this elastic response. Such oscillations have been detected up to 200 K, at least, by an anomalous broadening of the ^{87}Rb NMR line of $Rb_{0.3}MoO_3$.[44]

Finally, let us remark that from the knowledge of the x-ray diffuse scattering CDW correlation length and of the relevant frequencies of our neutron investigation (ν_A, v_φ, ν_K), it is possible to derive the microscopic parameters of the electron-phonon-coupled system at the basis of the Peierls instability of blue bronze. Such a determination can be found in Refs. 30 and 40. Here let us just mention that at 175 K the phason velocity v_φ is about one-tenth the Fermi velocity ($V_F \sim 1.9 \times 10^5$ m/s, deduced from the band calculation of Ref. 45). This gives a CDW reduced mass m^*/m_e of 80 (Ref. 33) according to[39]

$$\nu_\varphi = V_F \left[\frac{m_e}{m^*} \right]^{1/2} . \tag{7}$$

This mass enhancement is consistent with that of about 50 obtained in the vicinity of T_c by the use of the approximate formula[46]

$$\frac{m^*}{m_e} = 1 + \frac{16 k_B T \Delta(T)}{\pi (h \nu_A^0)^2} , \tag{8}$$

where at $T=175$ K ($T_c - 8$ K), $\Delta(T) \sim \Delta_0/2$,[20,23] with $2\Delta_0 \sim 0.1$ eV (Ref. 37) to 0.15 eV (Ref. 16) and where $\nu_A^0 = 1.7$ THz[7] (see also Fig. 7). This mass enhancement is also not too far from that deduced from millimeter-wavelength-range conductivity measurements.[32(b)] It is, however, more than 1 order of magnitude smaller than the one obtained in earlier infrared investigations.[9,10]

V. CONCLUSION

Our cold-neutron investigation of the CDW dynamics of the blue bronze $K_{0.3}MoO_3$ allows one to accurately study in frequency the Kohn anomaly and collective excitations of the phase and amplitude of the CDW for wave vectors propagating along the chain direction. This had not been possible in earlier studies of KCP,[13,14] probably because of the longer correlation length of the CDW fluctuations. We have been able to follow the temperature evolution of the characteristic frequencies of the dynamics of the Peierls instability and to observe, in particular, the underdamped regime of the Kohn anomaly. This study again had not been possible in KCP because of the intrinsic disorder of this material. The nearly complete softening observed places blue bronze in the displacive limit for the dynamics of its structural phase transition. Such a limit is expected for a classical Peierls transition. This behavior contrasts with that observed in TTF-TCNQ, for which there is nearly no pretransitional softening of the Kohn anomaly.[13,15] This difference is probably due to the importance of electron-electron interactions in the latter class of 1D organic conductors.[47] Finally, let us remark that our neutron findings are in perfect agreement with x-ray diffuse scattering results[27] for the Kohn anomaly softening, Raman data[7] for the frequency and damping of the amplitude mode, and millimeter-wavelength-range conductivity measurements[32(b)] for the pinning frequency of the phason.

ACKNOWLEDGMENTS

This work has benefitted from fruitful discussions with S. Barisic, C. Schlenker, and E. Tutis, and from collaboration with R. Currat and J. Marcus in the first neutron investigations of blue bronze. The Laboratoire de Physique des Solides is "Unité de Rechereche Associeé 2" au Centre National de la Recherche Scientifique No. 2.

[1]R. Comes, M. Lambert, H. Launois, and H. R. Zeller, Phys. Rev. B **8**, 571 (1973).

[2]B. Renker, L. Pintschovius, W. Glaser, H. Rietschel, R. Comes, L. Liebert, and W. Drexel, Phys. Rev. Lett. **32**, 836 (1974).

[3]For a recent review, see *Charge Density Waves in Solids,* Vol. 25 of *Modern Problems in Condensed Matter Science Series,* edited by L. P. Gork'ov and G. Gruner (Elsevier, New York, 1989).

[4]H. Cailleau, F. Moussa, C. M. E. Zeyen, and Y. Bouillot, Solid State Commun. **33**, 407 (1980).

[5]L. Bernard, R. Currat, P. Delamoye, C. M. E. Zeyen, S. Hubert, and R. de Kouchkovsky, J. Phys. C **16**, 433 (1983).

[6]E. F. Steigmeier, R. Loudon, G. Harbeke, H. Auderset, and G. Scheiber, Solid State Commun. **17**, 1447 (1975).

[7]G. Travaglini, I. Morke, and P. Wachter, Solid Commun. **45**, 289 (1983).

[8]P. Bruesch and H. R. Zeller, Solid State Commun. **14**, 1037 (1974).

[9]G. Travaglini and P. Wachter, Phys. Rev. B **30**, 1971 (1984).

[10]H. K. Ng, G. A. Thomas, and L. F. Schneemeyer, Phys. Rev. B **33**, 8755 (1986).

[11]See, for example, R. A. Cowley, Adv. Phys. **29**, 1 (1980).

[12]E. Tutis and S. Barisic, following paper, Phys. Rev. B **43**, 8431 (1991).

[13]R. Comes and G. Shirane, in *Highly Conducting One Dimensional Solids,* edited by J. T. Devreese, R. P. Evrard, and V. E. Van Doren (Plenum, New York, 1979), p. 17.

[14]K. Carneiro, G. Shirane, S. A. Werner, and S. Kaiser, Phys. Rev. B **13**, 4258 (1976).

[15]G. Shirane, S. M. Shapiro, R. Comes, A. F. Garito, and A. J. Heeger, Phys. Rev. B **14**, 2325 (1976).

[16]G. Travaglini, P. Wachter, J. Marcus, and C. Schlenker, Solid State Commun. **37**, 599 (1981).

[17]J. P. Pouget, S. Kagoshima, C. Schlenker, and J. Marcus, J. Phys. (Paris) Lett. **44**, L113 (1983).

[18]M. Sato, H. Fujishita, and S. Hoshino, J. Phys. C **16**, L877 (1983).

[19]T. Tamegai, K. Tsutsumi, S. Kagoshima, Y. Kanai, M. Tomozawa, M. Sato, K. Tsuji, R. Harada, M. Sakata, and T. Nakajima, Solid State Commun. **51**, 585 (1984); R. M. Fleming, L. F. Schneemeyer, and D. E. Moncton, Phys. Rev. B **31**, 899 (1985).

[20]J. P. Pouget, C. Noguera, A. H. Moudden, and R. Moret, J. Phys. (Paris) **46**, 1731 (1985) [**47**, 147(E) (1986)].

[21]C. Escribe-Filippini, J. P. Pouget, R. Currat, B. Hennion, and J. Marcus, in *Charge Density Waves in Solids,* Vol. 217 of *Lecture Notes in Physics,* edited by Gy. Hutiray and J. Sólyom (Springer-Verlag, Berlin, 1985), p. 71.

[22]J. P. Pouget, C. Escribe-Filippini, B. Hennion, R. Currat, A. H. Moudden, R. Moret, J. Marcus, and C. Schlenker, Mol. Cryst. Liq. Cryst. **121**, 111 (1985).

[23]M. Sato, M. Fujishita, S. Sato, and S. Hoshino, J. Phys. C **18**, 2603 (1985).

[24]J. Dumas, C. Schlenker, J. Marcus, and R. Buder, Phys. Rev. Lett. **50**, 757 (1983).

[25]K. Nomura, K. Kume, and M. Sato, J. Phys. C **19**, L289 (1986); A Janossy, C. Berthier, P. Segransan, and P. Butaud, Phys. Rev. Lett. **59**, 2348 (1987); J. Phys. (Paris) **51**, 59 (1990).

[26]S. Girault, A. H. Moudden, and J. P. Pouget, Phys. Rev. B **39**, 4430 (1989).

[27]J. P. Pouget, S. Ravy, and B. Hennion, in Proceedings of Transphase 3, Djerba, Tunisie, 19–24 March 1990 [Phase Transit. (to be published)].

[28]S. Girault, thesis, Orsay, 1987 (unpublished).

[29]W. J. Schutte and J. L. de Boer, Acta Crystallogr. B (to be published).

[30]J. P. Pouget, S. Girault, A. H. Moudden, B. Hennion, C. Escribe-Filippini and M. Sato, Phys. Scr. T **25**, 58 (1989).

[31]C. Escribe-Filippini, J. P. Pouget, B. Hennion, and M. Sato, Synth. Met. **19**, 931 (1987).

[32](a) G. Mihaly, Phys. Scr. **29**, 67 (1989); (b) T. W. Kim, D. Reagor, G. Gruner, K. Maki, and A. Virosztek, Phys. Rev. B **40**, 5372 (1989).

[33]These values correct those given in Ref. 40 where a factor 2π has been omitted in the velocities. The microscopic parameters derived in this reference are not affected by this omission.

[34]See, for example, Y. Nakane and S. Takada, J. Phys. Soc. Jpn. **54**, 977 (1985).

[35]The agreement does not hold for the damping constant: The ac conductivity measurements give an underdamped response (Ref. 32), while the $2k_F$ phason mode observed by neutron scattering is overdamped. Such a difference is due to the fact that these two kinds of measurement involve different correlation functions of the phase of the CDW [E. Tutis (private communication)].

[36]See, for example, M. J. Rice and S. Strassler, Solid State Commun. **13**, 1931 (1973).

[37]D. C. Johnston, Phys. Rev. Lett. **52**, 2049 (1984).

[38]E. Tutis and S. Barisic, Europhys. Lett. **8**, 155 (1989).

[39]P. A. Lee, T. M. Rice, and P. W. Anderson, Solid State Commun. **14**, 703 (1974).

[40]J. P. Pouget, in *Low Dimensional Electronic Properties of Molybdenum Bronzes and Oxides,* edited by C. Schlenker (Kluwer Academic, Dordrecht, 1989), p. 87.

[41]R. Brusetti, B. K. Chakraverty, J. Dumas, J. Devenyi, J. Marcus, and C. Schlenker, in *Recent Developments on Condensed Matter Physics,* edited by J. T. Devreese, L. F. Lemmens, V. E. Van Doren, and J. Van Royen (Plenum, New York, 1981), Vol. 2, p. 181.

[42]C. Berthier and P. Segransan, in *Low Dimensional Conductors and Superconductors,* Vol. 155 of *NATO Advanced Study Institute, Series B: Physics,* edited by J. Jerome and L. Caron (Plenum, New York, 1987).

[43]L. J. Sham, in *Highly Conducting One Dimensional Solids,* edited by J. T. Devreese, R. P. Evrard, and V. E. Van Doren (Plenum, New York, 1979), p. 227.

[44]P. Butaud, P. Segransan, C. Berthier, J. Dumas, and C. Schlenker, Phys. Rev. Lett. **55**, 253 (1985).

[45]M. H. Whangbo and L. F. Schneemeyer, Inorg. Chem. **25**, 2424 (1986).

[46]K. Maki and A. Virosztek, Phys. Rev. B **36**, 2910 (1987).

[47]S. Barisic, Mol. Cryst. Liq. Cryst. **119**, 413 (1985).